Sodium Channels in Planar Lipid Bilayers

Channel Gating Kinetics of Purified Sodium Channels Modified by Batrachotoxin

BERNHARD U. KELLER, ROBERT P. HARTSHORNE, JANE A. TALVENHEIMO, WILLIAM A. CATTERALL, and MAURICIO MONTAL

From the Departments of Biology and Physics, University of California at San Diego, La Jolla, California 92093, and the Department of Pharmacology, University of Washington, Seattle, Washington 98195

ABSTRACT Single channel currents of sodium channels purified from rat brain and reconstituted into planar lipid bilayers were recorded. The kinetics of channel gating were investigated in the presence of batrachotoxin to eliminate inactivation and an analysis was conducted on membranes with a single active channel at any given time. Channel opening is favored by depolarization and is strongly voltage dependent. Probability density analysis of dwell times in the closed and open states of the channel indicates the occurrence of one open state and several distinct closed states in the voltage (V) range -120 mV $\leq V \leq$ $+120$ mV. For $V \leq 0$, the transition rates between states are exponentially dependent on the applied voltage, as described in mouse neuroblastoma cells (Huang, L. M., N. Moran, and G. Ehrenstein. 1984. *Biophysical Journal.* 45:313–322). In contrast, for $V \geq 0$, the transition rates are virtually voltage independent. Autocorrelation analysis (Labarca, P., J. Rice, D. Fredkin, and M. Montal. 1985. *Biophysical Journal.* 47:469–478) shows that there is no correlation in the durations of successive open or closing events. Several kinetic schemes that are consistent with the experimental data are considered. This approach may provide information about the mechanism underlying the voltage dependence of channel activation.

INTRODUCTION

Voltage-sensitive sodium channels mediate the inward sodium current during the depolarizing phase of an action potential. A group of lipid-soluble toxins,

Address reprint requests to Dr. Mauricio Montal, Dept. of Neurosciences, Roche Institute of Molecular Biology, Nutley, NJ 07110. Dr. Keller's present address is Max-Planck-Institut für Biophysikalische Chemie, Göttingen, Federal Republic of Germany. Dr. Hartshorne's present address is Dept. of Pharmacology, Oregon Health Sciences University, Portland, OR 97201. Dr. Talvenheimo's present address is Dept. of Pharmacology, University of Miami School of Medicine, Miami, FL 33101.

J. GEN. PHYSIOL. © The Rockefeller University Press · 0022-1295/86/07/0001/23 $1.00

Volume 88 July 1986 1–23

batrachotoxin, veratridine, aconitine, and grayanotoxin, which share a common receptor site on the sodium channel, can profoundly alter the voltage and time dependence of opening, single channel conductance, ionic selectivity, and inactivation (reviewed by Catterall, 1980). Batrachotoxin (BTX), the most potent of these, shifts the voltage dependence of activation 50 mV in the hyperpolarizing direction and eliminates both fast and slow inactivation, which results in persistently open sodium channels at the normal membrane resting potential (Albuquerque et al., 1971; Narahashi et al., 1971; Khodorov and Revenko, 1979; Huang et al., 1982). Recently, single channel studies of BTX-modified sodium channels have extended our knowledge of sodium channel function (Quandt and Narahashi, 1982; Krueger et al., 1983; French et al., 1984; Moczydlowski et al., 1984) and have yielded a kinetic model of the BTX-modified sodium channel (Huang et al., 1984).

BTX and veratridine have also been extremely useful tools in the study of sodium channels that have been reconstituted into lipid vesicles after purification from rat muscle (Weigele and Barchi, 1982; Tanaka et al., 1983), rat brain (Talvenheimo et al., 1982; Tamkun et al., 1984), and eel electroplax (Rosenberg et al., 1984*a*). These studies have demonstrated that the sodium channel protein, which was purified on the basis of its ability to bind saxitoxin (STX) or tetrodotoxin (TTX), retains a functional ion conduction pathway with the ionic selectivity and neurotoxin sensitivity characteristic of the sodium channel. Single channel recordings of sodium channels purified from eel electroplax (Rosenberg et al., 1984*b*), rat brain (Hanke et al., 1984; Hartshorne et al., 1984, 1985), and rabbit T-tubules (Furman et al., 1986) were recently obtained as a first step toward the detailed characterization of the electrophysiological properties of the purified channel protein under voltage-clamp conditions. The voltage dependence of opening, the apparent gating charge, the voltage and concentration dependence of TTX block, the ionic selectivity, and the single channel conductance of BTX-modified sodium channels purified from rat brain were shown to be in good agreement with the properties of BTX-modified native rat brain sodium channels incorporated into planar lipid bilayers in a similar manner (Hartshorne et al., 1985; Krueger et al., 1983; French et al., 1984).

In this article, we determine the opening and closing rates and the voltage dependence of these rates for BTX-modified sodium channels purified from rat brain and reconsituted into planar lipid bilayers. These results are compared with an analysis of rate constants from a patch-clamp study of BTX-modified sodium channels in neuroblastoma cells (Huang et al., 1984), and kinetic models consistent with the data are discussed.

A preliminary account of this research has been presented elsewhere (Keller et al., 1985).

MATERIALS AND METHODS

Sodium Channel Purification and Reconstitution in Lipid Vesicles

Sodium channels were purified from a Triton X-100 solution of rat brain membranes by chromatography on DEAE-Sephadex, hydroxylapatite, and wheat germ agglutinin–Sepharose 4B, followed by sedimentation through sucrose gradients as described by Hartshorne

and Catterall (1984) using the modifications of Tamkun et al. (1984). The purified sodium channels had a specific activity of >2,000 pmol of [^{3}H]STX-binding sites per milligram of protein. The sodium channels were reconstituted using the procedure of Talvenheimo et al. (1982) into lipid vesicles composed of 35% (wt/vol) bovine brain phosphatidylethanolamine (PE) (Sigma Chemical Co., St. Louis, MO) and 65% bovine brain phosphatidylcholine (PC) (Sigma Chemical Co.) by adding a solution of 0.7% PE and 1.3% PC in 10% Triton X-100 to the purified channels to a final concentration of 0.2% PC and 0.105% PE. Thereafter, Triton X-100 was removed by overnight incubation with 0.25–0.4 ml of Bio-Beads SM-2 (Bio-Rad, Richmond, CA) per milliliter of reconstitution mixture. The Bio-Beads were removed and replaced with an equal volume of fresh Bio-Beads and the incubation was continued for an additional 2 h. The resulting vesicles were composed of 2 mg/ml PC, 1.05 mg/ml PE, 5–15 pmol/ml STX receptor, and ~17 μg protein/ml in 50 mM NaCl, 10 mM Hepes/Tris, pH 7.4, 0.5 mM $MgSO_4$, and 400 mM sucrose.

Reconstitution into Planar Lipid Bilayers

Sodium channels were incorporated into planar lipid bilayers (Hartshorne et al., 1985) by fusing vesicles with preformed bilayers (Krueger et al., 1983; Miller and Racker, 1976; Cohen et al., 1982; Weiss et al., 1984). Black lipid membranes (Mueller et al., 1963) were spread from a solution of 40 mg synthetic 1-palmitoyl-2-oleoyl PE and 10 mg/ml of 1-palmitoyl-2-oleoyl PC (Avanti Polar Lipids, Birmingham, AL) in *n*-decane or 50 mg/ml diphytanoyl PC (Avanti Polar Lipids) in *n*-decane across an aperture separating two aqueous compartments; the aperture diameter ranged between 70 and 200 μm. One compartment, identified here as the *cis* compartment, contained 450 μl of an aqueous solution of 0.5 M NaCl in medium I (10 mM Hepes/Na^+, pH 7.4, 0.15 mM $CaCl_2$, 0.1 mM $MgCl_2$, 0.05 mM EGTA) plus 1–5 μl of sodium channel proteoliposomes. The second (*trans*) compartment contained 450 μl of 0.2–0.4 M NaCl in medium I and 1 μM BTX. BTX was the generous gift of J. W. Daly (National Institutes of Health, Bethesda, MD). Bilayers with a specific capacitance between 0.26 and 0.34 $\mu F/cm^2$ and a resistance of >300 GΩ were used. After incorporation of a single sodium channel into the lipid bilayer, further incorporation was stopped by adding 4 M NaCl to the *trans* chamber to yield a final concentration of 0.5 M NaCl. All experiments were performed at 21 ± 2°C.

Electrical Recording and Data Analysis

A List Medical Electronics (Medical Systems Corp., Greenvale, NY) EPC-7 in the voltage-clamp mode was used to amplify the current and control the voltage across the bilayer through Ag/AgCl pellet electrodes. The *trans* electrode was set to a command voltage relative to the *cis* electrode, which was held at virtual ground. The EPC-7 output was filtered at 3 kHz and recorded on a Racal 4DS FM tape recorder (bandwidth DC to 5 kHz; Racal Recorders, Hythe, Southampton, England) for subsequent analysis. The recordings were filtered at 1–2 kHz with an eight-pole Bessel low-pass filter (Frequency Devices, Haverhill, MA) and digitized at a sampling interval of 100 μs on a PDP 11/34 computer (Digital Equipment Corp., Marlboro, MA). Channel open and closed conductance levels were discriminated using a pattern-recognition program described previously (Labarca et al., 1984). Only recordings with one active channel were analyzed. Analyzed data were transferred to a VAX 11/750 computer system (Digital Equipment Corp.) for further processing and fitting of different models.

Voltage Convention

The voltage convention used is the electrophysiological convention

$$V = V(\text{intracellular}) - V(\text{extracellular}).$$

The "extracellular" side of the sodium channel is defined as that from which TTX blocks (Narahashi et al., 1966) or is determined from the polarity of the electrode potential that closes the channel by hyperpolarization (Hartshorne et al., 1985).

Fitting of Models

Probability density analysis was used to identify the number of open and closed states of the channel and to determine the corresponding dwell time constants at different applied voltages. The hypothesis of a single-exponential component in the distributions of both open and closed dwell times was tested and rejected at $p \leq 0.05$ (χ^2 test). If the distributions were not well approximated by a single-exponential function, they were fitted with the sum of two exponential functions. The corresponding opening and closing rates are defined as the inverse of the closed and open dwell time constants. The transition rates between states (indicated by Greek letters) were fitted for different kinetic schemes.

C-O Scheme

For the kinetic scheme

$$\mathrm{C} \underset{\beta}{\overset{\alpha}{\rightleftarrows}} \mathrm{O}, \tag{1}$$

where C and O denote channel closed and open states, respectively, transition rates α and β must be determined. Considering a Markovian kinetic model, the measured opening and closing rates correspond to the eigenvalues λ_1 and λ_2 of the partitioned transition matrix (Colquhoun and Hawkes, 1981). Accordingly, the opening rate is

$$\lambda_1 = \alpha, \tag{2}$$

and the closing rate is

$$\lambda_2 = \beta. \tag{3}$$

The fraction of time in the open state is

$$f_{\mathrm{op}} = \frac{\alpha}{\alpha + \beta}. \tag{4}$$

C-C-O Scheme

For the kinetic scheme

$$\mathrm{C} \underset{\delta}{\overset{\gamma}{\rightleftarrows}} \mathrm{C} \underset{\beta}{\overset{\alpha}{\rightleftarrows}} \mathrm{O}, \tag{5}$$

a fit of four transition rates, α, β, γ, and δ, is required. Again, the measured opening and closing rates are given as the eigenvalues of the partitioned transition matrix. For the opening rates:

$$\lambda_1 = \tfrac{1}{2}[\alpha + \gamma + \delta + \sqrt{(\alpha + \gamma + \delta)^2 - 4\alpha\gamma}] \tag{6}$$

and

$$\lambda_2 = \tfrac{1}{2}[\alpha + \gamma + \delta - \sqrt{(\alpha + \gamma + \delta)^2 - 4\alpha\gamma}]; \tag{7}$$

for the closing rate:

$$\lambda_3 = \beta \tag{8}$$

(Colquhoun and Hawkes, 1981; Huang et al., 1984). The equations for the opening rates are simplified for $\lambda_1 \gg \lambda_2$. In this case, λ_1 approximates $\alpha + \gamma + \delta$, and λ_2 approximates $\alpha\gamma/\lambda_1$ (see Fig. 7*A*). Transition rate δ was determined from the fraction of time in the open state:

$$f_{op} = \alpha\gamma/(\alpha\gamma + \beta\gamma + \beta\delta). \tag{9}$$

C-O-C Scheme

For the kinetic scheme

$$C \underset{\beta}{\overset{\alpha}{\rightleftarrows}} O \underset{\delta}{\overset{\gamma}{\leftrightarrows}} C, \tag{10}$$

transition rates α, β, γ, and δ were named to underline the similarities with the C-C-O scheme. With λ_i as the eigenvalues of the partitioned transition matrix, the transition rates are given by

$$\lambda_1 = \alpha, \tag{11}$$

$$\lambda_2 = \gamma \tag{12}$$

for the opening rates and

$$\lambda_3 = \beta + \delta \tag{13}$$

for the closing rate. The fraction of time in the open state is

$$f_{op} = \alpha\gamma/(\alpha\gamma + \beta\gamma + \alpha\delta). \tag{14}$$

C-C-O-C-C Scheme

The transition rates for the scheme

$$C_1 \underset{\delta}{\overset{\gamma}{\rightleftarrows}} C_2 \underset{\beta}{\overset{\alpha}{\rightleftarrows}} O \underset{\beta'}{\overset{\alpha'}{\leftrightarrows}} C_3 \underset{\delta'}{\overset{\gamma'}{\leftrightarrows}} C_4 \tag{15}$$

were determined separately by splitting it into a C-C-O scheme and an O-C-C scheme for negative and positive applied voltages, respectively. The four transition rates for each voltage range were calculated as described previously for the C-C-O scheme. The fraction of time in the open state is

$$f_{op} = \alpha\gamma\alpha'\gamma'/[\alpha'\gamma'(\alpha\gamma + \beta\gamma + \beta\delta) + \alpha\gamma(\beta'\gamma' + \beta'\delta')]. \tag{16}$$

Fitting of Transition Rates

In general, all types of fits correspond to physical models involving dipole moments of varying voltage dependence (Hodgkin and Huxley, 1952; Neher and Stevens, 1979; French and Horn, 1983; Horn and Vandenberg, 1984; Vandenberg and Horn, 1984). For all models, the variation is expressed as the standard error of the mean, unless otherwise specified. For the physical models invoking the movement of gating charges, exponential functions of voltage were fitted to all transition rates according to the equation:

$$\text{transition rate} = \nu e^{\left[\frac{(a+bV)}{kT}\right]}, \tag{17}$$

where k is the Boltzmann constant, T is the absolute temperature, and ν is the effective

vibration frequency (in units of reciprocal seconds). The logarithm of the rates as a function of voltage was fitted by a linear least-squares program using the RS/1 software package of BBN Research Systems (Bolt, Beranek and Newman, Inc., Cambridge, MA) on a VAX 11/750 computer system.

For models other than that involving freely moving gating charges, the opening and closing rates were fitted with more complex functions of voltage. In particular, rates were fitted with the function

$$\text{transition rate} = \nu \frac{1}{1 + e^{\left[\frac{-(a+bV)}{kT}\right]}}, \tag{18}$$

where a and b are constants. This is a sigmoidal function that saturates at transition rate = 0 and transition rate = a. This type of function was used by Hodgkin and Huxley (1952) to approximate the transition rate between the inactivated and the open states. Fitting was achieved in a series of iterations, in which the parameters were systematically adjusted by the Marquardt-Levenberg method until a least-squares solution was reached (Fletcher, 1971). Rate constants that could not be fitted by this function were approximated by using a Taylor expansion for their voltage dependence. In this case, no specific assumptions about the underlying molecular mechanisms were made. As described by Neher and Stevens (1979), the transition rates were approximated by the series

$$\text{transition rate} = \nu e^{\left(\frac{a+bV+cV^2+\cdots}{kT}\right)} \tag{19}$$

with constants a, b, c, ... The fitting was done by plotting the log transition rate and using the Marquardt-Levenberg algorithm to fit a polynomial according to least squares.

RESULTS

Single Channel Records: Channel Gating Is Voltage Dependent

Fig. 1*A* shows single channel currents at the indicated applied voltages from a purified, BTX-modified sodium channel reconstituted in a lipid bilayer. Negative (hyperpolarizing) voltages favor channel closing, whereas positive (depolarizing) voltages favor channel opening. The gating kinetics of five different sodium channels were determined from ~30-s-long recordings of data similar to those in Fig. 1*A* for each applied voltage between −120 and +120 mV.

Probability Density Analysis: Closed Dwell Time Histograms and the Opening Rates

Fig. 1*B* illustrates a section of a single channel current recording obtained at −95 mV (top panel) and the corresponding computer-generated signal produced by the pattern-recognition program that measures open and closed times (lower panel). The accurate reproduction of the actual data produced by the program indicates the fidelity of the assignment of "closed" and "open" states and the transitions between the two states. These parameters are stored and then used for the probability density analysis. The distributions of closed dwell times are determined by plotting the number of channel closings t units long as a function

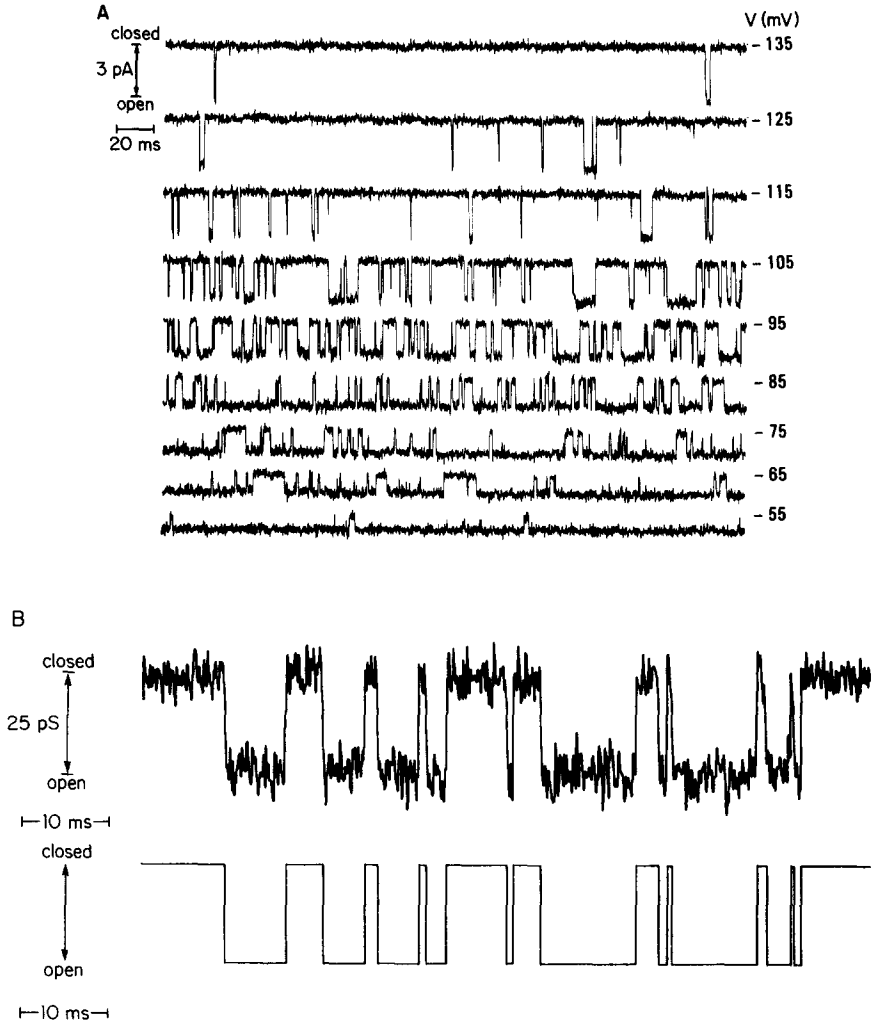

FIGURE 1. Voltage dependence of sodium channel gating. (*A*) A single *trans*-facing sodium channel was incorporated into a diphytanoyl PC bilayer formed across a 70-μm aperture bathed in 0.5 M NaCl medium I (*cis*) and 0.2 M NaCl medium I plus 1 μM BTX (*trans*). The current was recorded under voltage-clamp conditions while the voltage was changed in 10-mV steps lasting 1 min from −135 to −55 mV. The current records were filtered at 1 kHz, converted to digital form at a sampling frequency of 5 kHz, and plotted at reduced speed on a Gould 2200 S chart recorder (Gould, Inc., Cleveland, OH). (*B*) The upper record is a computer-digitized signal recorded at an applied volume of $V = -95$ mV under same conditions as in *A*. After filtering at 2 kHz, the records were digitized at a sampling interval of 100 μs. A downward deflection is a channel opening event and the next upward step is associated with channel closing. Transitions between the closed and open states are indicated by the arrows. The lower record is the reconstruction of the signal by a pattern-recognition computer program (Labarca et al., 1984).

of t. These dwell time histograms are fitted by a probability density function of the form

$$f(t) = \sum_{i=1}^{N} a_i e^{-t/\tau_i}, \tag{20}$$

where a, the amplitude of the fitted curve and τ, the time constant of the exponential fit, are calculated by a χ^2 minimization algorithm (Fletcher, 1971; Labarca et al., 1985). The goodness of fit is measured by the probability (p) of obtaining a value for χ^2 that is greater than or equal to the obtained value. A $p \leq 0.05$ indicates a significant disagreement between the experimental histogram and the fitted probability density. Fig. 2 is a graphic presentation of dwell times in the open and closed states of the sodium channel at $V = -95$, -85, and -65 mV, for a typical experiment. The fitted probability density (smooth curve) is superimposed on the experimental histogram.

Table I displays the results of the analysis of closed dwell time histograms for two different applied voltages. At $V = -100$ mV, the closed dwell time distribution is well fitted by a single-exponential function ($p > 0.05$). This holds for applied voltages more negative than -75 mV. In contrast, at $V \geq -75$ mV, the closed times are not well fitted by a single exponential ($p = 0.00$ at $V = -65$ mV), and the sum of two exponentials is required to fit the histograms.

Table II shows the parameters of the probability density function for three different experiments. Note that A_i corresponds to the relative area under the fitted curve. The average short closed time decreases markedly with depolarization from $\tau_{C_1} = 25.2 \pm 6.2$ ms (SEM, $n = 5$) at $V = -100$ mV to $\tau_{C_1} = 1.8 \pm 1.1$ ms ($n = 5$) at $V = -60$ mV. The variability of the dwell times for each applied voltage reflects the earlier observations (Hartshorne et al., 1985) that the voltage dependence of channel opening varies from channel to channel. The corresponding opening rate (closed time^{-1}) is plotted as a semilogarithmic function of the applied voltage in Fig. 3*A*. The fast opening rate is exponentially voltage dependent for negative applied voltages with a slope of 13.5 ± 0.9 mV/e-fold change.

In contrast, the long closed time (τ_{C_2}), apparent only at applied voltages more positive than -75 mV, is prolonged by depolarization. The corresponding slow opening rate (Fig. 3*A*) decreases exponentially with a slope of -20.2 ± 2.3 mV/e-fold change ($n = 5$).

For positive applied voltages, closed dwell time histograms are not well fitted by a single-exponential function. The sum of two exponential functions is required to fit the data. The average closed times at $V = +100$ mV are $\tau'_{C_1} = 0.79 \pm 0.09$ ms ($n = 3$) and $\tau'_{C_2} = 26.8 \pm 3.1$ ms ($n = 3$). The corresponding opening rates are practically voltage independent, increasing e-fold for voltage changes of >300 mV (Table III).

Open Dwell Time Histograms and Closing Rates

For all applied voltages investigated, the open dwell time histograms are well fitted by a single exponential (Fig. 2; Tables I and II). Depolarization prolongs the open time constants from $\tau_O = 1.4 \pm 0.3$ ms at $V = -100$ mV to $\tau_O = 28.4 \pm 4.5$ ms at $V = -60$ mV. At negative applied voltages, closing rates (= open times^{-1}) are exponentially voltage dependent with a slope of -13.6 ± 0.6 mV/e-

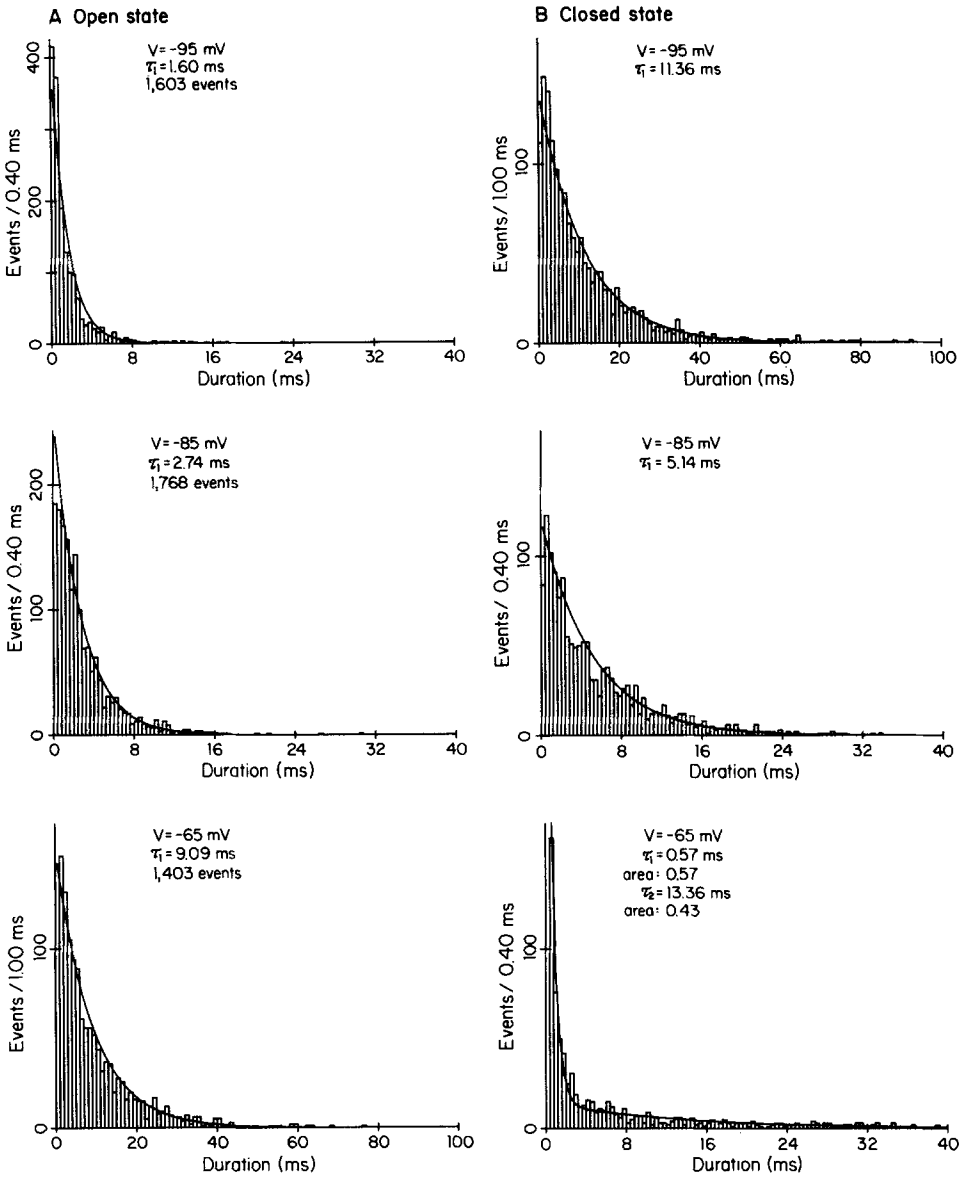

FIGURE 2. Probability density analysis of dwell times in the open (*A*) and closed (*B*) states of the sodium channel. The applied voltages were −95 (top panel), −85 (middle panel), and −65 (lower panel) mV. For purposes of illustration, the data were sampled in sampling units of 0.4 or 1 ms, as indicated. The fitted curves (smooth curve) were superimposed on the histograms of the actual data (bars). With the exception of the closed dwell time histogram at $V = -65$ mV, all the data were well fitted by a single exponential, ignoring dwell times $t \leq 0.1$ ms. For the graphic demonstration of the bimodal distribution at $V = -65$ mV, dwell times $t \leq 0.5$ ms were ignored, thereby increasing the relative area of the "slow" exponential component. The parameters of the exponential components and the number of events analyzed are indicated.

TABLE I

Number of Exponential Components

State	Voltage	Number of exponentials	Degrees of freedom	χ^2	p
	mV				
Closed	−100	1	347	1.07	0.22
	−65	1	195	1.87	0.00
		2	193	0.75	0.99
Open	−100	1	166	0.97	0.57
	−65	1	456	0.96	0.69

fold change (Fig. 3*B*). In contrast, for positive applied voltages, the closing rate is only moderately voltage dependent (71 ± 26 mV/e-fold change).

Probability of Channel Opening

Fig. 4 shows the fraction of time that the channel spends in the open state as a function of the applied voltage. For applied voltages between −100 and −50 mV, the probability of channel opening is strongly voltage dependent. The voltage at which the channel is open 50% of the time, V_{50}, is −82 mV for this channel. For applied voltages more positive than 50 mV, the channel stays open 95% of the time. The function displayed in Fig. 4 is a fundamental property of the system: it can be calculated by integration of conductance histograms as previously described (Hartshorne et al., 1985; open squares, Fig. 4), or alternatively from dwell time histograms (solid circles) according to:

$$f_{op} = N\tau_O/T, \tag{21}$$

where N is the number of transitions and T is the total recording time at a particular applied voltage. The agreement demonstrates that the time constant τ_O is accurately determined by our procedures and justifies the assumption that

TABLE II

Parameters of Exponential Components

Voltage	Experiment number	N	Number of exponentials	Open state			Closed state					
				A_O	τ_O	p	A_{C_1}	τ_{C_1}	p	A_{C_2}	τ_{C_2}	p
mV					*ms*			*ms*			*ms*	
−100	1	953	1	1.0	1.34	0.03	1.0	16.56	0.12	—	—	—
−108	2	1,139	1	1.0	1.80	0.14	1.0	37.53	0.99	—	—	—
−96	3	1,152	1	1.0	1.33	0.19	1.0	9.64	0.81	—	—	—
−80	1	2,458	1	1.0	6.25	0.17	1.0	4.51	0.72	—	—	—
−88	2	878	1	1.0	8.00	0.46	1.0	10.20	0.17	—	—	—
−76	3	1,664	1	1.0	6.12	0.79	1.0	2.62	0.16	—	—	—
−60	1	635	1	1.0	26.27	0.99	1.0	0.78	0.00	—	—	—
−68	2	1,720	1	1.0	16.03	0.98	1.0	3.42	0.02	—	—	—
−56	3	654	1	1.0	49.28	0.99	1.0	0.74	0.00	—	—	—
−60	1	635	2	—	—	—	0.92	0.45	—	0.08	13.31	0.58
−68	2	1,720	2	—	—	—	0.85	3.16	—	0.15	13.14	0.35
−56	3	654	2	—	—	—	0.96	0.55	—	0.04	9.38	0.34

the residence time in the open state is independent of the transition that leads to the open state, which is characteristic of a Markov process (Feller, 1971).

Covariance Analysis

Single channel recordings contain information conducive to identifying the number of kinetic open and closed states, to determining the rates of transitions

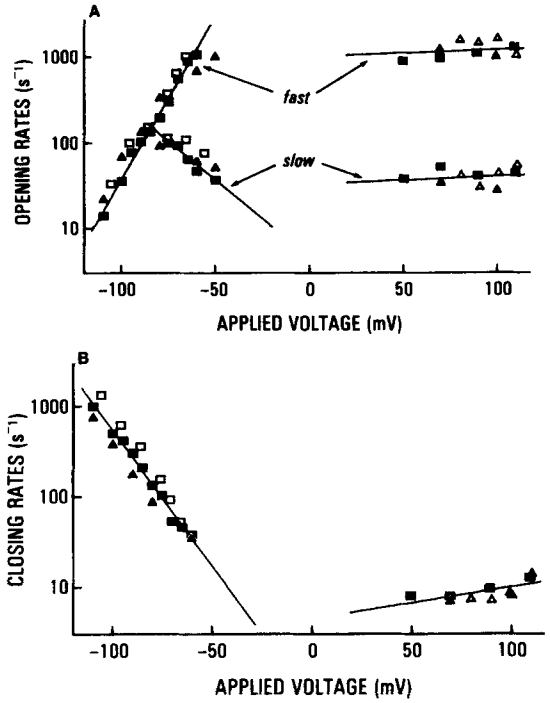

FIGURE 3. Voltage dependence of opening (*A*) and closing rates (*B*). (*A*) Current records similar to those in Fig. 1, lasting 30–60 s at each voltage, were digitized, and the opening rates at each applied voltage were determined by probability density analysis. The different symbols correspond to data points obtained from four different membranes. To prevent noise from interfering with the determination of channel transitions, only records for applied voltages $V < -50$ mV or $V > 50$ mV were analyzed. For applied voltages $V < -80$ mV, the data were well fitted by a single opening rate. For applied voltages more positive, the hypothesis of a single opening rate was rejected at a $p = 0.05$ significance level (χ^2 test). For all voltages, the data were well fitted by the assumption of two opening rates. For negative applied voltages, the opening rates were found to be strongly voltage dependent, whereas for positive applied voltages they were practically voltage independent. The straight lines were obtained by fitting different exponential functions to the four opening rates according to a least-squares fit. (*B*) Two exponentially voltage-dependent closing rates fitted the data for all applied voltages investigated. The fits were done as in *A*. For negative applied voltages, the rate was strongly voltage dependent, whereas for positive applied voltages the rate was almost voltage independent. The different symbols indicate data points obtained from four different experiments.

TABLE III

Transition Rates

Transition rates	mV/e-fold change	Rate at $V = -70$ mV
		s^{-1}
α	13.5±0.9 ($n = 5$)	477±118
β	−13.6±0.6 ($n = 5$)	63±14
γ	−20.2±2.3 ($n = 5$)	139±44
δ	18.6±3.5 ($n = 4$)	40±13
		Rate at $V = +100$ mV
α'	855±282 ($n = 3$)	1,273±154
β'	71±26 ($n = 3$)	9.0±.45
γ'	325±125 ($n = 3$)	37.2±4.2
δ'	438±153 ($n = 3$)	285.5±67.3

between these states, and to establishing the pathways by which these states are communicated. One way of extracting information about the transition routes between open and closed states is to calculate the covariance function of single channel transitions as described by Labarca et al. (1985). Covariance functions, which can be readily estimated from experimental data, have provided information that has proved valuable in discriminating between different kinetic models of the cholinergic receptor channel and the chloride channel of *Torpedo californica* (Labarca et al., 1985).

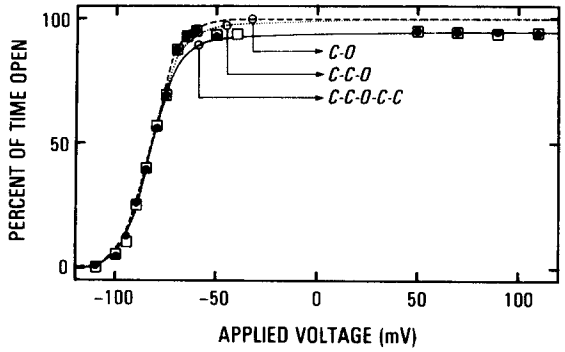

FIGURE 4. Probability of channel opening. The percentage of time that the channel spends in the open state is strongly voltage dependent for applied voltages -100 mV $< V < -50$ mV. For positive applied voltages, the channel spends 95% of the time in the open state. The open squares were obtained by integrating conductance histograms as described in Hartshorne et al. (1985). The solid circles were calculated independently for different applied voltages according to Eq. 21: $f_{op} = N\tau_O/T$. The three lines correspond to different kinetic models of sodium channel gating and were calculated from the rate constants obtained for the best fit of the data to the models (see text for details). For models with exponentially voltage-dependent transition rates, only the five-state C-C-O-C-C model fits the data for negative and positive applied voltages.

Briefly, if T_1, T_2, T_3, . . . T_n is a sequence of successive channel open dwell times, the covariance function is given by:

$$\Gamma(k) = 1/(n - k) \sum_{i=1}^{n-k} (T_i - T)(T_{i+k} - T), \tag{22}$$

where T is the average open time for this sequence. The corresponding correlation function $\hat{\rho}(k)$ is a "normalized" covariance function [i.e., $\rho(0) = 1$] and is calculated from

$$\hat{\rho}(k) = \Gamma(k)/\Gamma(0). \tag{23}$$

As described by Fredkin et al. (1985), the correlation function $\hat{\rho}(k)$ provides information about the minimum number of transition pathways between the open and closed states.

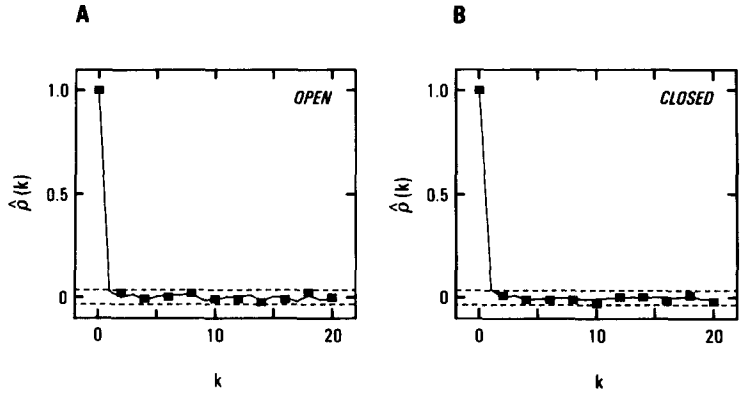

FIGURE 5. Autocorrelation function. (*A*) Autocorrelation function for the open aggregate of the purified sodium channel at an applied voltage $V = -60$ mV. The squares are the result of an experiment with $N = 3{,}578$ transitions. The dashed lines are $\pm 2\sqrt{N}$, which corresponds to ± 2 times the approximate standard error of the estimate in the case of white noise. The line displays the average autocorrelation function for four different experiments. In no case is there a significant correlation in the sequence of open times. (*B*) Autocorrelation function for the closed aggregate at an applied voltage $V = -60$ mV. The symbols and lines correspond to Fig. 6. Although the distribution of closed dwell times shows two exponential components, there is no correlation in the sequence of closing events.

Sequence of Open Times

The correlation function of sodium channel open times is shown in Fig. 5*A* for an applied voltage $V = -60$ mV. The solid line is the average for four different experiments and the square data points display the result for a recording with $N = 3{,}578$ transitions. For all $k > 0$, the correlation function has a value smaller than $\pm 2\sqrt{N}$, i.e., ± 2 times the approximate standard error of the estimate in the case of white noise (dashed line). This result indicates that there is no significant correlation in the durations of successive open dwell times.

Sequence of Closed Times

Fig. 5*B* shows the correlation function for successive closed dwell times at an applied voltage $V = -60$ mV. There is no correlation in the durations of successive closing events. This result is particularly important for data that display two closed time constants, namely, recordings obtained at V more positive tham -75 mV.

The results of the covariance analysis are consistent with any kinetic model that postulates a single open state (Labarca et al., 1985). Since covariance functions are calculated independently from the probability density functions of open and closed dwell times, the results of covariance analysis support the postulate of a single open state as inferred from the distribution functions.

DISCUSSION

In discussing the experimental data, we consider first the kinetic models used to determine the transition rates, and then we outline plausible physical mechanisms that can generate the observable values, namely, lifetimes in channel closed and open states.

Two-State Model

For applied voltages more negative than $V = -75$ mV, open and closed dwell time histograms are well fitted by a single-exponential function. The minimum kinetic scheme consistent with the data considers one closed and one open state (Eq. 1):

$$\mathrm{C} \underset{\beta}{\overset{\alpha}{\rightleftarrows}} \mathrm{O}.$$

Transition rates α and β correspond to the inverse of the closed and open dwell times. The fast opening rate, α, and the closing rate, β, at $V < 0$ mV are exponential functions of voltage. In this simple two-state model, the probability of occurrence of each state depends exponentially on the energy of that state and the extent to which is is affected by the applied electric field. The fraction of time in the open state, f_{op}, calculated for the least-squares fit, is shown as a dashed line in Fig. 4 (C-O model). This is formally equivalent to fitting the fraction in the open state with a Boltzmann function (French et al., 1984):

$$f_{op} = 1/[1 + e^{q(V-V_{50})/kT}], \tag{24}$$

where k is the Boltzmann constant, T is the absolute temperature, and q is the apparent gating charge. This function matches the dashed line in Fig. 4 for 3.9 electronic charges and $V_{50} = -82$ mV. Thus, for the purified sodium channel, the gating charge q can be attributed to $q_\alpha = 2.0$ charges determining the voltage dependence of α, and $q_\beta = 1.9$ charges determining the voltage dependence of β.

The simple two-state model with exponentially voltage-dependent transition rates approximates the kinetics of BTX-modified sodium channels exhibited at negative applied voltages. However, it does not account for either the occurrence of the second closed state or the additional channel states at positive applied voltages.

Three-State Models

C-C-O model. For applied voltages greater than −75 mV, closed time histograms are not well fitted by a single-exponential function. This indicates the existence of another closed state. A linear chain of one open and two closed states was shown to account for the kinetic scheme of native BTX-modified sodium channels in neuroblastoma cells (Eq. 5):

$$C \underset{\delta}{\overset{\gamma}{\rightleftarrows}} C \underset{\beta}{\overset{\alpha}{\rightleftarrows}} O$$

(Huang et al., 1984). The fraction of time in the open state is given by Eq. 9:

$$f_{op} = \alpha\gamma/(\alpha\gamma + \beta\gamma + \beta\delta).$$

As described by Huang et al. (1984), exponentially voltage-dependent transition rates are fitted to the measured opening and closing rates (Fig. 6). Transition

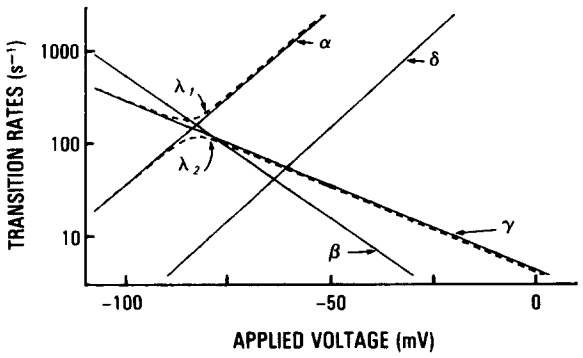

FIGURE 6. C-C-O model with exponentially voltage-dependent transition rates. For the C-C-O scheme, the measured opening rates (Fig. 3*A*) correspond to eigenvalues λ_1 and λ_2 of the transition matrix (Huang et al., 1984) and are related to the transition rates α, γ, and δ as described in Materials and Methods. For voltages other than −80 mV, the eigenvalues λ_1 and λ_2 approximate the transition rates α and γ. Transition rate β is equal to the measured closing rate. δ was calculated using Eq. 9 for the percentage of time in the open state and the data of Fig. 4 for $V < 0$ mV. All transition rates were fitted to exponential functions of voltage by the least-squares method. The data used for the fitting are shown as solid squares in Fig. 3 and as solid circles in Fig. 4. The results of the fitting for all experiments investigated are displayed in Table III.

rate α is exponentially voltage dependent, with a slope of 13.5 ± 0.9 mV/e-fold change ($n = 4$), which corresponds to ~2 apparent gating charges moving through the membrane electric field. Transition rate β has an opposite voltage dependence with approximately the same slope (−13.6 ± 0.6 mV/e-fold change, $n = 5$). Transition rate γ has a similar voltage dependence with an e-fold change for −20.3 ± 2.3 mV ($n = 5$). This slope corresponds to 1.2 apparent gating charges sensing the applied electric field. For transition rate δ, determined from the fraction of time in the open state (Eq. 9), the least-squares fit is obtained for a slope of 18.6 ± 3.5 mV/e-fold change ($n = 4$).

To test this model, the fraction of time in the open state is calculated for the transition rates. The result is shown as a dotted line in Fig. 4 (C-C-O model). Note that the experimental data are well approximated by the C-C-O model, but only for negative applied voltages.

This analysis indicates that the three-state C-C-O model with exponentially voltage-dependent transition rates accounts for all the data on channel kinetics at negative applied voltages, but is inadequate for positive applied voltages.

C-O-C model. We now consider a different kinetic scheme with one open and two closed states, where the open state is accessed directly from the closed states (Eq. 10):

$$C \underset{\beta}{\overset{\alpha}{\rightleftarrows}} O \underset{\delta}{\overset{\gamma}{\rightleftarrows}} C.$$

The fit of the transition rates, α, β, and γ, is performed as described for the C-C-O scheme. The key difference from the C-C-O scheme appears in the voltage dependence of transition rate δ. For the C-O-C scheme, the least-squares exponential fit for δ decreases with positive voltage (-8.0 ± 1.3 mV/e-fold change). Thus, if this model were correct, both rates γ and δ, between the open and the right closed state, would decrease with positive voltage. The result for the fraction of time in the open state is equivalent to that for the C-C-O model (Fig. 4).

For the BTX-activated sodium channel, the results of both the probability density analysis and the covariance analysis are consistent with the C-O-C model. Thus, with these analyses, the C-O-C and C-C-O schemes cannot be distinguished. To identify the correct scheme, voltage jump relaxation measurements will be required.

Five-State Model

C-C-O-C-C model. Transition rates are determined by splitting the C_1-C_2-O-C_3-C_4 scheme into a C_1-C_2-O scheme for negative and an O-C_3-C_4 scheme for positive applied voltages. This approximation is justified for the BTX-modified sodium channel, because channel states C_1 and C_2 occur only at negative applied voltages, whereas states C_3 and C_4 occur only at positive applied voltages. For the negative and the positive voltage range, the transition rates are determined separately.

The least-squares fit for the transition rates is shown in Fig. 7. The transition rates for $V < 0$ mV correspond to the previously determined C-C-O scheme. The data for $V > 0$ mV are fitted to an O-C-C kinetic scheme as previously described for negative applied voltages (Huang et al., 1984). With the exception of β' (71 mV/e-fold change), every transition rate requires a voltage difference of >300 mV for an e-fold change (corresponding to <0.08 apparent gating charges crossing the membrane).

The percentage of time in the open state is calculated by assuming that all the transition rates of Fig. 7 hold for applied voltages -120 mV $< V <$ 120 mV. Eq. 16 is used to calculate the fraction of time that the channel spends in the open state (solid line in Fig. 4). The five-state model with exponentially voltage-dependent transition rates accounts for the percentage of time in the open state for the complete voltage range studied (Fig. 8*A*).

Thus, for negative and positive applied voltages, the data fit a kinetic scheme with one open and four kinetically distinct closed states. Channel gating at negative applied voltages is determined by a voltage-dependent mechanism (C-C-O scheme), whereas for positive applied voltages it is governed by a voltage-independent mechanism (O-C-C scheme).

C-C-O model with saturating rate constants. In the five-state model, there is a striking symmetry between the channel states at negative and positive applied voltages: the exponentially voltage-dependent transition rates at negative applied voltages seem to level off at positive voltages (Fig. 3). It is therefore tempting to speculate that the voltage-dependent C-C-O scheme at negative applied voltages is transformed into the voltage-independent O-C-C scheme at positive applied

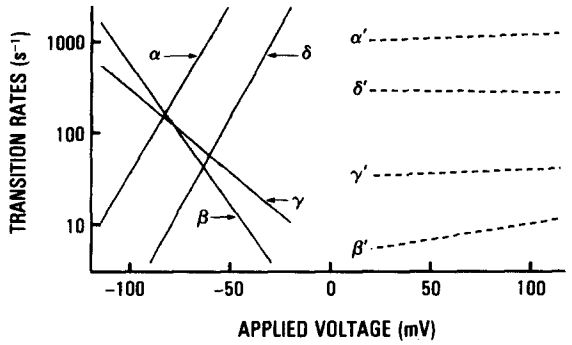

FIGURE 7. C-C-O-C-C model with exponentially voltage-dependent transition rates. The transition rates for negative applied voltages were fitted as described in Fig. 6. For positive applied voltages, the data were fitted to an O-C-C scheme (see Materials and Methods). The five-state kinetic model with exponentially voltage-dependent transition rates fits all the data.

voltages. Without any assumptions about the underlying molecular mechanism, the simplest approach is to approximate the voltage dependence of the transition rates for $-120\ \text{mV} < V < +120\ \text{mV}$ with an exponential series of the form (Eq. 19):

$$\text{transition rate} = \nu e^{\left(\frac{a+bV+cV^2+\cdots}{kT}\right)}$$

(Neher and Stevens, 1979), where a, b, c, . . . are constants. This function is used to describe the voltage dependence of the closing rate, β, and the slow opening rate, γ, for the complete voltage range investigated. For transition rates α and δ, the number of parameters is reduced by using Eq. 18:

$$\text{transition rate} = \nu \frac{1}{1 + e^{\left[\frac{-(a+bV)}{kT}\right]}}$$

(Hodgkin and Huxley, 1952), where a and b are constants. In fact, this function is a special case of Eq. 19 that explicitly includes a saturation of the transition rate. The relative occurrence of channel states for the C-C-O model with

saturating transition rates is shown in Fig. 8*B*. The result of the fitting procedure for the voltage dependence of transition rates α, β, γ, and δ in the voltage range $-120 \text{ mV} < V < +120 \text{ mV}$ is displayed in Fig. 9.

It is evident, therefore, that the gating of BTX-modified sodium channels is

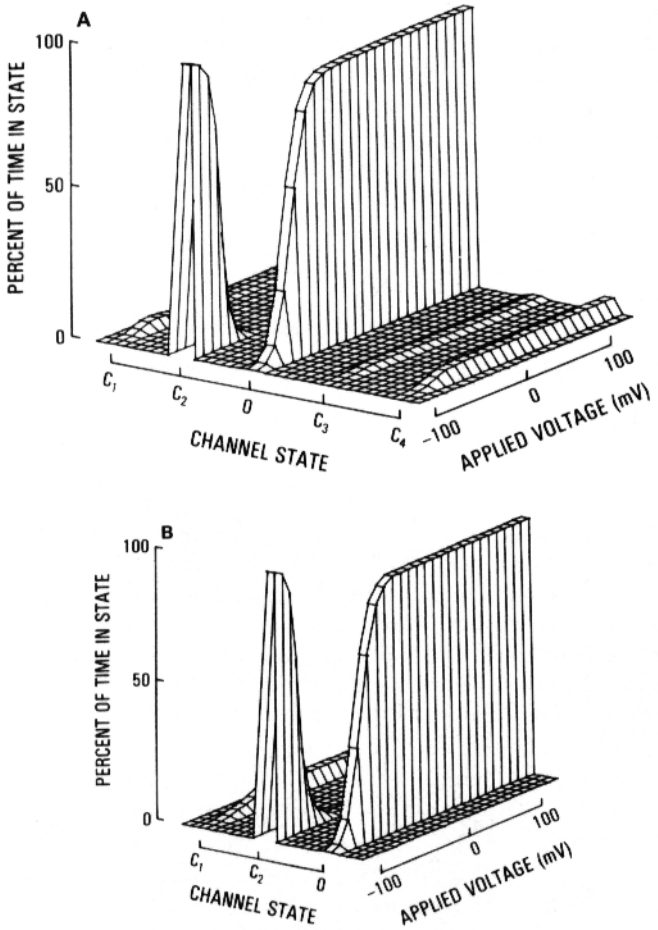

FIGURE 8. Occurrence of channel states as a function of voltage for two kinetic schemes of the BTX-modified sodium channel. (*A*) Percentage of time in different states is plotted vs. channel state and applied voltage for the C-C-O-C-C model. The fractions of time in different states were determined by assuming exponentially voltage-dependent rate constants as displayed in Fig. 7 and standard chemical kinetics under steady state conditions. Note that the open state, O, and the second closed state, C_2, are by far the most occupied states. (*B*) Percentage of time in different states for the C-C-O model with saturating transition rates. f_{op} was calculated using Eq. 9 and the values of the voltage-dependent transition rates shown in Fig. 9. Variations of f_{op} for $-50 \text{ mV} \leq V \leq +50 \text{ mV}$ were eliminated by plotting the mean f_{op} for $V > -50$ mV. The fractions of time in channel states C_1 and C_2 were determined in the same way.

also well described with a single C-C-O scheme with saturating transition rates. Physical models that could generate saturating transition rates include the displacement of a charged gating particle in and out of the membrane electric field or the neutralization by counter-charges for positive applied voltages.

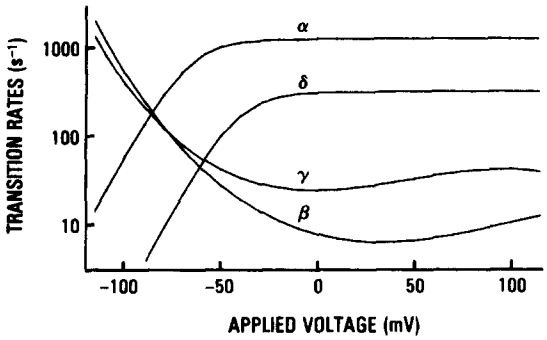

FIGURE 9. C-C-O scheme with saturating rate constants. Rate α was fitted to the function

$$\alpha = \nu \frac{1}{1 + e^{\left[\frac{-(a+bV)}{kT}\right]}}.$$

In a series of iterations, the parameters ν, a, and b were systematically adjusted until a least-squares solution was reached. The constant ν is the effective vibration frequency and was found to be 1,251 s^{-1} for transition rate α. The physical meaning of constant a is the energy barrier that determines channel opening at negative applied voltages and it is fitted with a value of 6.11 kT. Constant $b = 2.34$ electronic charges and corresponds to the apparent gating charge in the negative voltage range. Transition rate δ was fitted with the same function with constants $\nu = 313$ s^{-1}, $a = 4.36$ kT, $b = 2.3$ electronic charges. Transition rate β was approximated by the function

$$\beta = \nu e^{\left(\frac{a+bV+cV^2+dV^3}{kT}\right)}$$

with $\nu = 1$ s^{-1} and constants a, b, c, and d. The least-squares fit was obtained for $a = 2.0$ kT, $b = -0.32$ electronic charges, $c = 228\ kT/V^2$, and $d = -714\ kT/V^3$. The physical meaning of a is the energy barrier that determines channel closing and b is the apparent gating charge at 0 mV. Constants c and d characterize the modification of the gating mechanism induced by the applied electric field. Transition rate γ was fitted with the same function with constants $a = 3.2$ kT, $b = +0.01$ electronic charges, $c = 168\ kT/V^2$, and $d = -1{,}179\ kT/V^3$. The data used for the fitting were the same as in Fig. 7. A summary of these results is shown in Table III.

For the entire studied range of applied voltages, BTX-modified sodium channel gating can be explained by a C-C-O-C-C model with exponentially voltage-dependent transition rates (Fig. 8*A*) or by a C-C-O model with saturating transition rates (Fig. 8*B*). At present, we favor the latter scheme because of its inherent simplicity.

Comparison of the Native and Purified Sodium Channel

The kinetic analysis of the purified sodium channel modified by BTX suggests a scheme with one open and two closed states with exponentially voltage-dependent transition rates between states for negative applied voltages. This result is in agreement with the kinetic scheme proposed for the native sodium channel in mouse neuroblastoma cells (Huang et al., 1984) as summarized in Table IV. Some details deserve further comment.

(*a*) The similar voltage dependences of α, β, and γ indicate that the same number of gating charges are involved in the gating process. (*b*) For the purified sodium channel, the absolute value of α at $V = -70$ mV is sixfold faster (Table III; Table I of Huang et al., 1984). (*c*) From the similarity of β in native and purified sodium channels, the inference can be drawn that the energy levels of

TABLE IV

Transition Rates for a C-C-O Model of the Native and the Reconstituted Na^+ Channel

Transition rate	Native channel*	Reconstituted channel‡
	mV/e-fold change	*mV/e-fold change*
α	10.98 ($n = 4$)	13.5 ($n = 5$)
β	−18.96 ($n = 5$)	−13.6 ($n = 5$)
γ	−25.80 ($n = 2$)	−20.2 ($n = 5$)
δ	9.5 ($n = 1$)	18.6 ($n = 4$)

* Data of Huang et al. (1984) from neuroblastoma sodium channels (average, n = number of experiments).

‡ Sodium channels purified from rat brain.

the open state are equal for the two kinds of channels. (*d*) For transition rate δ, the agreement is only qualitative because δ is more voltage dependent for the purified channel. As δ primarily determines P_{max}, the maximum percent of time in the open state at negative applied voltages, the difference in δ is reflected in $P_{max} = 95\%$ for the purified sodium channel and $P_{max} = 80\%$ for the native sodium channel. It is worth noting that Krueger et al. (1983) determined the P_{max} for native sodium channels in planar lipid bilayers to be $\geq 98\%$.

Disparities in channel gating characteristics may arise from differences in lipid and ionic environments. For example, the gating kinetics of alamethicin channels are significantly slower in natural membranes than in lipid bilayers (Sakmann and Boheim, 1979). Similarly, opening rate α is significantly slower for the native sodium channel in neuroblastoma cells than for the purified channel investigated in planar lipid bilayers. Specifically, the purified sodium channel was studied in symmetric solutions of 0.5 M NaCl in neutral lipid membranes. By contrast, the native channel was investigated in 0.1 M salt in the natural membrane milieu, which, in general, is partially negatively charged. The influence of ionic strength and lipid composition on channel gating is an interesting area for future studies (cf. Weiss et al., 1984).

It is clear, therefore, that native and purified sodium channels can be described in terms of the same kinetic scheme. This further supports the notion that the

purified sodium channel protein retains its functional properties after reconstitution (Hartshorne et al., 1985).

The kinetic analysis presented here will serve as a basis to characterize the effect of other drugs, toxins, or biochemical and genetic protein modifications on channel gating. This approach may provide insights into the relationship between sodium channel structure and the voltage dependence of channel activation.

We are indebted to J. Rice, R. Horn, E. Neher, L. Y. M. Huang, and G. Ehrenstein for their perceptive comments, Tony Lee for computer programming, and Laura Castrejon for her valuable assistance.

This research was supported by grants from the National Institutes of Health (EY-02084) and the Department of the Army Medical Research (17-82-C-2221). R. Hartshorne was a Postdoctoral Fellow of the National Multiple Sclerosis Society.

Original version received 8 November 1985 and accepted version received 24 March 1986.

REFERENCES

Albuquerque, E. X., J. W. Daly, and B. Witkop. 1971. Batrachotoxin: chemistry and pharmacology. *Science.* 172:995–1002.

Catterall, W. A. 1980. Neurotoxins that act on voltage sensitive sodium channels in excitable membranes. *Annual Review of Pharmacology and Toxicology.* 20:15–43.

Cohen, F. S., M. A. Akabas, and A. Finkelstein. 1982. Osmotic swelling of phospholipid vesicles causes them to fuse with planar phospholipid bilayer membranes. *Science.* 217:458–460.

Colquhoun, D., and A. G. Hawkes. 1981. On the stochastic properties of single ion channels. *Proceedings of the Royal Society of London B Biological Sciences.* 211:205–235.

Feller, W. 1971. An Introduction to Probability Theory and Its Applications. Vol. II. John Wiley & Sons, New York. 669.

Fletcher, R. A. 1971. A modified Marquardt subroutine for non-linear least squares. *AERE Report R6799.*

Fredkin, D. R., M. Montal, and J. A. Rice. 1985. Identification of aggregated Markovian models: application to the nicotinic acetylcholine receptor. *In* Proceedings of the Berkeley Conference in Honor of Jerzy Neyman and Jack Kiefer. Lucien M. Le Cam and Richard A. Olshen, editors. Wadsworth Publishing Co., Belmont, CA. 1:269–289.

French, R. J., and R. Horn. 1983. Sodium channel gating: models, mimics, and modifiers. *Annual Review of Biophysics and Bioengineering.* 12:319–356.

French, R. J., J. F. Worley III, and B. K. Krueger. 1984. Voltage-dependent block by saxitoxin of sodium channels incorporated into planar lipid bilayers. *Biophysical Journal.* 45:301–310.

Furman, R. E., J. C. Tanaka, P. Mueller, and R. L. Barchi. 1986. Voltage-dependent activation in purified reconstituted sodium channels from rabbit T-tubular membranes. *Proceedings of the National Academy of Sciences.* 83:488–492.

Hanke, W., G. Boheim, J. Barhanin, D. Pauron, and M. Lazdunski. 1984. Reconstitution of highly purified saxitoxin-sensitive Na^+-channels into planar lipid bilayers. *European Molecular Biology Organization Journal.* 3:509–515.

Harshorne, R. P., and W. A. Catterall. 1984. The sodium channel from rat brain. Purification and subunit composition. *Journal of Biological Chemistry.* 259:1667–1675.

Hartshorne, R. P., B. U. Keller, J. A. Talvenheimo, W. A. Catterall, and M. Montal. 1984. Functional reconstitution of the purified brain sodium channel in planar lipid bilayers. *Society for Neuroscience Abstracts.* 10:864.

Hartshorne, R. P., B. U. Keller, J. A. Talvenheimo, W. A. Catterall, and M. Montal. 1985. Functional reconstitution of the purified brain sodium channel in planar lipid bilayers. *Proceedings of the National Academy of Sciences.* 82:240–244.

Hodgkin, A. L., and A. F. Huxley. 1952. A quantitative description of membrane current and its application to conduction and excitation in nerve. *Journal of Physiology.* 117:500–544.

Horn, R., and C. A. Vandenberg. 1984. Statistical properties of single sodium channels. *Journal of General Physiology.* 84:505–534.

Huang, L. M., N. Moran, and G. Ehrenstein. 1982. Batrachotoxin modifies the gating of sodium channels in internally perfused neuroblastoma cells. *Proceedings of the National Academy of Sciences.* 79:2082–2085.

Huang, L. M., N. Moran, and G. Ehrenstein. 1984. Gating kinetics of batrachotoxin-modified sodium channels in neuroblastoma cells determined from single-channel measurements. *Biophysical Journal.* 45:313–322.

Keller, B. U., R. P. Hartshorne, J. A. Talvenheimo, W. A. Catterall, and M. Montal. 1985. Gating kinetics of purified sodium channels from rat brain modified by batrachotoxin in planar lipid bilayers. *Biophysical Journal.* 47:439*a*. (Abstr.)

Khodorov, B. I., and S. V. Revenko. 1979. Further analysis of the mechanism of action of batrachotoxin on the membrane of myelinated nerve. *Neuroscience.* 4:1315–1330.

Krueger, B. K., J. F. Worley III, and R. J. French. 1983. Single sodium channels from rat brain incorporated into planar lipid bilayer membranes. *Nature.* 303:172–175.

Labarca, P., J. Lindstrom, and M. Montal. 1984. Acetylcholine receptor in planar lipid bilayers. Characterization of the channel properties of the purified nicotinic acetylcholine receptor from *Torpedo californica* reconstituted in planar lipid bilayers. *Journal of General Physiology.* 83:473–496.

Labarca, P., J. Rice, D. Fredkin, and M. Montal. 1985. Kinetic analysis of channel gating: application to the cholinergic receptor channel and to the chloride channel from *Torpedo californica. Biophysical Journal.* 47:469–478.

Miller, C., and E. Racker. 1976. Ca^{2+} induced fusion of fragmented sarcoplasmic reticulum with artificial bilayers. *Journal of Membrane Biology.* 30:283–300.

Moczydlowski, E., S. Hall, S. Garber, G. Strichartz, and C. Miller. 1984. Batrachotoxin-activated Na^+ channels in planar lipid bilayers. Competition of tetrodotoxin block by Na^+. *Journal of General Physiology.* 84:687–704.

Mueller, P., D. O. Rudin, H. T. Tien, and W. C. Wescott. 1963. Methods for the formation of single bimolecular lipid membranes in aqueous solution. *Journal of Physical Chemistry.* 67:534–535.

Narahashi, T., N. C. Anderson, and J. W. Moore. 1966. Tetrodotoxin does not block excitation from inside the nerve membrane. *Science.* 153:765–767.

Narahashi, T., T. Deguchi, and E. X. Albuquerque. 1971. Effects of batrachotoxin on nerve membrane potential and conductances. *Nature.* 229:221–222.

Neher, E., and C. F. Stevens. 1979. Voltage-driven conformational changes in intrinsic membrane proteins. *In* The Neurosciences. Fourth Study Program. MIT Press, Cambridge, MA. 623–629.

Quandt, F. N., and T. Narahashi. 1982. Modification of single Na-channels by batrachotoxin. *Proceedings of the National Academy of Sciences.* 79:6732–6736.

Rosenberg, R. L., S. A. Tomiko, and W. S. Agnew. 1984*a*. Reconstitution of neurotoxin-modulated ion transport by the voltage-regulated sodium channel isolated from the electroplax of *Electrophorus electricus. Proceedings of the National Academy of Sciences.* 81:1239–1243.

Rosenberg, R. L., S. A. Tomiko, and W. S. Agnew. 1984*b*. Single-channel properties of the reconstituted voltage-regulated Na-channel isolated from the electroplax of *Electrophorus electricus*. *Proceedings of the National Academy of Sciences.* 81:5594–5598.

Sakmann, B., and G. Boheim. 1979. Alamethicin-induced single channel conductance fluctuations in biological membranes. *Nature.* 282:336–339.

Talvenheimo, J. A., M. M. Tamkun, and W. A. Catterall. 1982. Reconstitution of neurotoxin-stimulated sodium transport by the voltage-sensitive sodium channel purified from rat brain. *Journal of Biological Chemistry.* 257:11868–11871.

Tamkun, M. M., J. A. Talvenheimo, and W. A. Catterall. 1984. The sodium channel from rat brain: reconstitution of neurotoxin-activated ion flux and scorpion toxin binding from purified components. *Journal of Biological Chemistry.* 259:1676–1688.

Tanaka, J. C., J. F. Eccleston, and R. L. Barchi. 1983. Cation selectivity characteristics of the reconstituted voltage-dependent sodium channel purified from rat skeletal muscle sarcolemma. *Journal of Biological Chemistry.* 258:7519–7526.

Vandenberg, C. A., and R. Horn. 1984. Inactivation viewed through single sodium channels. *Journal of General Physiology.* 84:535–564.

Weigele, J. B., and R. L. Barchi. 1982. Functional reconstitution of the purified sodium channel protein from rat sarcolemma. *Proceedings of the National Academy of Sciences.* 79:3651–3655.

Weiss, L. B., W. N. Green, and O. S. Andersen. 1984. Single channel studies on the gating of batrachotoxin modified sodium channels in planar lipid bilayers. *Biophysical Journal.* 45:67*a*. (Abstr.)